Realistic Air Filter Media Performance Simulation. Part I: Navier-Stokes / Finite-Volume CFD Procedures

HVAC&R Research
Publication details, including instructions for authors and subscription information:
http://www.tandfonline.com/loi/uhvc20

Realistic Air Filter Media Performance Simulation: Part I: Navier-Stokes / Finite-Volume CFD Procedures

Paolo Tronville PhD [a] , Bin Zhou PhD [b] & Richard Rivers [c]

[a] Department of Energy - Politecnico di Torino, Corso Duca degli Abruzzi 24, I-10129, Turin, Italy Phone: +39 011 0904477 Fax: +39 011 0904477

[b] College of Urban Construction and Safety Engineering, Nanjing University of Technology, Nanjing, China

[c] EQS Inc, Louisville, Kentucky, U.S.A.

Accepted author version posted online: 15 Apr 2013.

To cite this article: HVAC&R Research (2013): Realistic Air Filter Media Performance Simulation: Part I: Navier-Stokes / Finite-Volume CFD Procedures, HVAC&R Research

To link to this article: http://dx.doi.org/10.1080/10789669.2013.795464

Realistic Air Filter Media Performance Simulation:

Part I: Navier-Stokes / Finite-Volume CFD Procedures

Corresponding Author:

Paolo Tronville (PhD, ASHRAE Member)

Department of Energy - Politecnico di Torino

Corso Duca degli Abruzzi 24

I-10129 Turin

Italy

Telephone: +39 011 0904477

Fax: +39 011 0904499

E-mail: paolo.tronville@polito.it

Co-Authors:

Bin Zhou (PhD)

College of Urban Construction and Safety Engineering,

Nanjing University of Technology

Nanjing, China

E-mail: zhoubinwx@gmail.com

Richard Rivers (ASHRAE Fellow)

EQS Inc., Louisville, Kentucky U.S.A.

E-mail: rdrivers@bellsouth.net

A review of published studies of numerical techniques for air filter performance simulation shows that there are two general approaches to such simulations. One describes gases flowing through filter media as continuous fluids, influenced by the macro properties viscosity, density and pressure. The alternate approach treats gases as molecules in random motion, impacting their own kind and solid surfaces on a micro scale. The appropriate form for a given filter medium and operating condition depends on the gas properties and the Knudsen number (Kn) of the smallest fibers in the filter medium simulated. When no fiber Kn exceeds 0.01, the Navier-Stokes equation and finite-volume solutions should simulate filter media pressure drop and particle capture reliably, if correct particle and fiber boundary conditions, including "slip" at boundaries, are employed. In addition, fibrous media geometry must be modeled in enough detail to make simulation results match experimental data. This Part I of our paper reviews literature related to filter media flow and particle capture simulation in the continuum regime, using the finite-volume method for flow calculations. We suggest appropriate boundary conditions and parameter values. Part II of this paper discusses media simulation in flow regimes where other equations and computation techniques must be used.

INTRODUCTION

Fibrous-media air filters may contain fibers with diameters ranging from a few nanometers to more than 50 micrometers. Particles captured by such media have similar diameter ranges. Computational fluid dynamics (CFD) modeling of the flow and particle capture in filter media has problems: the mean free path of the molecules in the gas may be of the same order of magnitude as the diameters of the filter media fibers or the particles to be captured. A high value of this ratio can occur when the gas pressure is low, giving large mean free paths, or when the immersed bodies - fibers and particles - are small. In either case, the probability of impacts between gas and surface molecules is greatly reduced from the continuous-fluid, or “continuum”, condition. Thermodynamic equilibria of momentum and temperature between the fiber and particle surfaces and the gas are not reached. A salient result of this is the phenomenon of “slip”.

With continuum flow and relatively large bodies, the gas flow velocity at the solid boundary reaches the same velocity as the boundary; “zero-slip” or “no-slip” boundary conditions exist. At very low pressures or with immersed-body dimensions in the order of a tenth of the mean free path of the gas molecules, behavior is completely discontinuous, and gas molecule impacts with the boundary are far less frequent. This is “free molecular flow”, the regime where full slip occurs. The condition between the two limits, with partial slip, is “transitional flow”.

For the continuum flow regime, the Navier-Stokes equations reliably predict flow and particle capture if the filter medium geometry is accurately described and correct boundary conditions are used. If a significant fraction of the fibers in the simulated medium are operating in the non-continuum regime, the resulting flow pattern will appear reasonable, but the details of the flow near small fibers are not properly modeled, and pressure drops and particle capture will

not be reliably predicted. Part II of this paper considers alternate approaches for simulations beyond the continuum regime. Here, we consider only the Navier-Stokes equation using the finite-volume method.

We will attempt to identify the most reliable choices for boundary conditions based on results of existing filter media simulations which include experimental verification. We limit the discussion to isothermal conditions and the relatively low media gas velocities existing in air filter applications. With these restrictions, gas flows will always be viscous, devoid of turbulence, and “incompressible”, meaning free of shock phenomena. We ignore gravity, convection, or any other external forces on the gas flows. Electrostatically charged media are not considered, but the effects of the minimal charges carried by aerosols that have reached the Boltzmann equilibrium state are included.

SIMULATION OF FIBROUS MEDIA GEOMETRIES

Most fibrous media geometries are described reasonably well as assemblies of cylindrical fibers with uniform or random fiber diameters. Simulations of such media have been performed using both 2-dimension and 3-dimension models. 3D models are inherently more complex than 2D, and require far more computational power and time. 3D models should mimic the actual geometry of media better than 2D, but the complexity of 3D has usually forced users to simplifications such as using a limited number of straight, uniform-diameter fibers. A 2D model essentially represents a planar cross-section of a small portion of the filter media, cut perpendicular to the entering face of the medium. Such a cross-section would in fact intersect the

fibers at random angles, and show the fiber cross-sections as ellipses with random eccentricities. A common simplification is to imagine that the fibers are all parallel to each other and to the face of the medium, and that the fiber cross-sections can then be represented by circles. Figure 1 shows a CFD computation domain based on this model. The diameter distribution of the circles in the domain is made to match the measured distribution of fiber diameters, and the circles located at random positions within the domain. The domain represents the entire thickness of the medium (between X=0 and X=L), and a relatively narrow width W. The number of circles in the area $L \cdot W$ is chosen so that the sum of the circle areas equals the fractional volume of solids in the actual medium. Thus the space available for gas flow in the 2D domain is in the same proportion as the space available in the actual medium. Empty spaces are provided upstream and downstream of the fiber bed to simulate such spaces in the test duct. The entrance velocity V_{in} is set constant across the domain width. At the downstream boundary X_{out}, the usual boundary conditions choice is that the x-partial derivative of pressure is zero, $\delta P/\delta x = 0$. The boundaries for Y=0 and Y=W are set as "periodic", which eliminates any y-component of gas velocity across these boundaries.

FLOW REGIMES AND KNUDSEN NUMBER

Knudsen numbers are essential in defining filter media performance. For the basic flow equation to describe flow throughout a given filter medium, the choice of the equation depends on the Knudsen number of the fiber with the smallest characteristic dimension. For a cylinder the Knudsen number is:

$$Kn = \frac{\lambda}{d} \quad (1)$$

where λ is the mean free path of the gas molecules and d a characteristic dimension of the cylinder. Most filter fibers are circular cylinders, with d the fiber diameter. Some are approximately rectangular ribbons, in which case d is probably best taken as the width of the ribbon. For fibers with other cross-sections, the hydraulic diameter is a suitable choice for d. However, filter media with non-circular fiber cross-sections will usually have uniform cross-section dimensions throughout a given filter medium, hence can be modeled with their actual geometry and random fiber locations, as has been done for fibers with circular cross-sections. CFD studies of media having non-circular fibers are included in Table 4.

No exact *Kn* values divide flow regimes. Table 1, a modification of one in Yun and Agarwal (2002), divides the flow regimes into sections, with appropriate computational methods listed for each. The *Kn* bounds here represent a consensus of values found in our literature survey.

MOMENTUM EXCHANGE

Molecular Interaction in Gases

In a gas at rest, the (vector) velocities of its molecules are completely random, and the sum of these at any point averaged over time is zero. If the gas is flowing, there are additions to the vector velocities of the individual molecules such that their sum, averaged, equals the

(vector) bulk flow velocity. Functions for gas macro properties (viscosity, thermal conductivity and temperature) are obtained by summing the *change* in powers of the vector velocities of all molecules arriving at the collision point with random directions but defined velocity distributions. Viscosity prediction depends on molecular momentum change, which is proportional to velocity. Thermal conductivity prediction depends on change in energy, which is proportional to velocity squared. The relations between single-molecule collisions and macro gas properties thus depend in part on the velocity distributions of the gas molecules.

Molecular dynamics techniques have improved theory-based prediction accuracy of thermophysical properties, but expressions derived from experimental data provide the most reliable values. These should be used when making flow simulations. Bird et al (2002) and Poling et al (2002) are comprehensive sources for fluid thermophysical properties, and general texts on transport phenomena, such as Chapman and Cowling (1970), Bird (1994) and Lucas (1997) are useful in understanding gas molecular dynamics.

Interaction of Gas Molecules with Surfaces

The behavior of a gas molecule near a solid surface and during and after collision with a surface is far more complicated than collision with other molecules of its own kind. For our purposes, it will be sufficient to understand the meaning and relationships of the terms slip coefficient and tangential momentum accommodation coefficient (TMAC), without exploring the derivation of these coefficients from the dynamics of single molecules. In the continuum flow regime, for analysis purposes, one can imagine that gas molecules striking the surface adopt

the same vector velocity as the surface. This is the no-slip or zero-slip condition. In addition, the gas at the boundary is assumed to take on the temperature of the surface. Between this layer and the bulk gas for normal gases there is a velocity gradient and viscous stress, dependent on the derivative of the tangential gas velocity, the derivative being taken in the direction normal to the surface.

Under other conditions, molecules striking the surface will not reach either momentum or thermal equilibrium with the surface. Their average tangential velocity and temperature adjusts only partially to the surface velocity and temperature. The bulk gas at the boundary will have motion relative to the moving or stationary boundary. This is the "slip" or "partial-slip" boundary condition. This condition can exist when the gas pressure is small, and too few molecular impacts per unit time to reach equilibrium, or when the object immersed in the fluid is so small that the number of impacts on a given area is erratic in time.

Maxwell proposed that under conditions of partial or complete slip, which is true for all real gases, the difference between the gas molecule and solid wall tangential velocities (u_g and u_{sw}) at the boundary is:

$$u_g - u_{sw} = \frac{2-s}{s}\lambda \frac{du}{dn}\Big|_w \qquad (2)$$

Here $\frac{du}{dn}\Big|_w$ is the absolute value at the wall of the rate of velocity change in the direction normal to the wall. Factor s is proportional to what is now called the tangential momentum accommodation coefficient (TMAC) for the combination of gas and surface. The TMAC, σ_{tma}, is:

$$\sigma_{tma} = \left(u_{in} - u_{rf}\right) / \left(u_{in} - U_w\right) \qquad (3)$$

Where

u_{in} = the sum of the tangential components of gas molecular incident momenta at the wall;

u_{rf} = the sum of the tangential components of gas momenta for molecules rebounding or "reflected" from the wall;

U_w = the tangential component of the solid wall momentum.

The value of σ_{tma} ranges from 0 for zero-slip conditions (Kn ~ 0) to 1 for full-slip (Kn >10). Expressions with additional terms have been developed, giving better models of molecular momentum interchange and hence computed flow patterns. Equation 2 is often suggested as the appropriate boundary condition for Navier-Stokes analysis with partial slip. However, Barber et al (2004) show that the correct expression for *curved* boundaries is, for the 2D case in Cartesian coordinates:

$$u_g - u_{sw} = \frac{2-\sigma_{tma}}{\sigma_{tma}} \lambda \left(\frac{\partial u_x}{\partial y} + \frac{\partial u_y}{\partial x} \right) \Big|_w \qquad (4)$$

The boundary condition for the 3D case is more complicated. Urquiza et al (2008), Zhao (2009), Krivodonova and Berger (2006), and Kirkpatrick et al (2003) all discuss the implications of boundary conditions for curved boundaries. Values of TMACs are discussed in the Gas Properties section below.

GOVERNING EQUATIONS

Navier-Stokes Equation

It is possible to simulate the random impacts of individual molecules in a gas or against a surface, and sum the vector components to determine the resulting bulk motion of a fluid. Molecular-dynamics simulations do this. However, even at 0.01 atmosphere pressure, the immense number of molecules per unit gas volume prohibits computation for complex geometries.

Early numerical simulations of complex gas flows were based on differential equations derived from thermodynamic principles to describe flowing gases conceived as continuous fluids. Governing equation derivation begins with the behavior of a "control volume" in the moving fluid. This is a portion of the gas small enough that the change in fluid properties (density, velocity) across it can be approximated by linear functions. For the "incompressible", isothermal conditions we consider, two equations are required to describe the instantaneous state of this control volume:

a. The continuity equation, giving the fluid mass entering and leaving the volume (Equation 5);
b. An equation describing the rate of momentum change (Equation 6).

Partial differential equations (PDEs) can be written, expressing the velocity and density of the control volume as a function of time and the gas properties. Various assumptions can simplify the equations and more accurately describe flows at specific geometry scales and operating conditions. The PDEs can be defined for one, two or three dimensions, and any convenient coordinate system. One set of simplifying assumptions leads to the Navier-Stokes equation (7):

$$\nabla \bullet \mathbf{v} = 0 \qquad (5)$$

$$\rho_g\left(\frac{\partial \mathbf{v}}{\partial t} + \mathbf{v} \bullet \nabla \mathbf{v}\right) = -\nabla p + \mu \nabla^2 \mathbf{v} \qquad (6)$$

Substitution of Equation (5) in Equation (6) gives:

$$\rho_g \frac{\partial \mathbf{v}}{\partial t} = -\nabla p + \mu \nabla^2 \mathbf{v} \qquad (7)$$

For CFD calculations, Equation 7 is first transformed into its components in a coordinate system convenient for the geometry analyzed. For filter simulation, Cartesian coordinates are convenient. A 2D analysis will be expressed in the *x*- and *y* components of **v**, using symbols v_1 and v_2; a 3D analysis uses the *x*-,*y* and *z* components of **v**, and symbols v_1, v_2 and v_3**.** The component equations are then converted into algebraic equation sets with discrete small time and space steps, allowing numerical solutions by CFD computer codes. Boundary conditions must be defined and mesh generated for the geometry analyzed. Both commercial and open-source CFD codes provide these procedures, along with gas properties, appropriate boundary-value expressions for the continuum-flow regime, and graphic presentations of calculated results. Details appear in many textbooks on CFD, and user manuals for commercial and open-source CFD codes (see for instance www.cfd-online.com).

Fiber boundary conditions and particle-tracking algorithms supplied by the CFD code may be inadequate, and need to be replaced by the user. CFD runs must be made in a range of progressively finer mesh scales to demonstrate that the solution obtained is independent of mesh scale. Some condition may exist in the flow pattern that the equation solvers cannot resolve. This possibility with “conventional” CFD has led many investigators to prefer the more robust LB and DSMC methods even for continuum flow.

BOUNDARY CONDITIONS

Domain Boundaries

The computational domain must include a zone upstream of the section representing the medium, for simulation of gas flow approaching the medium, and a zone downstream also. The width of the domain needs to be enough to simulate an average portion of the medium. At the domain inlet ($x = 0$) the boundary condition is $\mathbf{v} = V_0$, a constant "face velocity" for the medium, here parallel to the x-axis. At the discharge end of the domain a reliable condition is $\delta p/\delta x=0$ for all y and z. Along the sides of the domain the "reflection" or "symmetry" boundary condition is set. This forces the rate of change of the normal components of the vectors at the boundary to be zero, minimizing the influence of the boundary, while confining the flow to the domain.

Fiber Boundaries

Regardless of the level of slip, at all solid boundaries the normal component of gas velocity must be zero, because the boundary is not penetrated. The tangential component is also zero for continuum flow, for there is no slip, and the boundary is at rest for filter media geometries. With slip, things change. For fibers with rectangular cross-section, the flat-boundary tangential velocity is given by Equation 2, with $u_{sw} = 0$ and $s = \sigma_{tma}$. For fibers with circular cross-sections, and where binders are simulated, Equation 4 or its 3D equivalent must be used.

SIMULATION OF AEROSOL PARTICLE CAPTURE

When the flow field has been calculated, one can calculate the tracks of particles through the fiber bed until they collide with a fiber or previously captured particle, or pass downstream. Aerodynamic drag and diffusion properties of spheres are well-established, and much work has been done on the behavior of other particle shapes, such as ellipsoids, short cylinders and agglomerates of smaller particles.

For filter media, gravity is ignored (since filter media can operate in any orientation) but Brownian motion included, at least for smaller particles. Also, particle drag may need to include particle boundary slip. Regardless of how the flow field is obtained, there are two different methods to simulate particle behavior: Lagrangian and Eulerian.

Lagrangian Particle Tracking

The Lagrangian method assumes that particles are imaginary point objects: they do not alter the flow. Forces on particles, however, do depend on the reality of their finite diameters, their mass, and, when they strike a fiber, their elastic and adhesive properties. With these assumptions, particle motion before contact with a fiber is determined by setting the rate of momentum change equal to aerodynamic drag:

$$\frac{\pi}{6}\rho_p d_p^3 \frac{d\left(\mathbf{v}_p - \mathbf{v}_g\right)}{dt} = -\frac{3\pi\mu d_p \left(\mathbf{v}_p - \mathbf{v}_g\right)}{C_C} \qquad (8)$$

Here d_p, ρ_p and $\mathbf{v}_p$ are particle diameter, density and (vector) velocity, and μ, ρ_g and $\mathbf{v}_g$ gas viscosity, density, and (vector) velocity. C_C is Cunningham's correction for particle slip, discussed below. For calculation, Equation 8 must be discretized into component equations, two for 2D analyses and three for 3D. Brownian motion is incorporated by adding a term to Equation 8:

$$\frac{\pi}{6}\rho_p d_p^3 \frac{d\left(\mathbf{v}_p - \mathbf{v}_g\right)}{dt} = -\frac{3\pi\mu d_p\left(\mathbf{v}_p - \mathbf{v}_g\right)}{C_C} + \frac{\pi}{6}\rho_p d_p^3 K_B \delta_{ij} P_B \qquad (9)$$

Where

$$K_B = \left(\frac{216\mu kT}{(\Delta t)\pi\rho_p\rho_g d_p^5\left(\rho_p/\rho_g\right)^2 C_C}\right)^{0.5} \qquad (10)$$

Here

k is Boltzmann's Constant;

T is the absolute temperature;

Δt is the time-step used in the discretized CFD equation;

δ_{ij} is Kronecker's delta, which is expressed in terms of the subscripts i,j in the component equations derived from Equation 9 by $\delta_{ij} = 1$ if i=j, $\delta_{ij} = 0$ if i≠j;

P_B is a set of random numbers with the Gaussian (normal) distribution, having mean = 0 and variance = 1.

In effect, δ_{ij} sets the direction of the path change from each Brownian impulse, and P_B the relative magnitudes of the velocities imparted, hence the distances traveled in time Δt.

Zhao et al (2011) and Aliabadi and Rogak (2011) debated the validity of the Lagrangian approach for particle *Kn* above about 0.2, concluding that the Lagrangian particle tracking

algorithm in some Navier-Stokes CFD codes is invalid. Their discussion shows that reasonable agreement of any CFD result with experimental data is needed before extending the method used to other simulations, such as particle loading, or to different operating conditions. In addition, CFD requires procedures to guarantee that results are meaningful from a purely mathematical standpoint. These procedures are called CFD verification and validation. Standard procedures are defined in AIAA (1998). A tutorial on the subject is at: www.grc.nasa.gov/WWW/wind/valid/tutorial/tutorial.html.

Eulerian Particle Tracking

The Eulerian method treats the particles as a *separate gas phase*, a cloud with finite dimensions, and particle concentration *C*. The aerosol cloud is interspersed with the gas flow at the upstream boundary of the computational domain. Thereafter particle concentration is described by Equation 11:

$$\frac{\partial \rho C}{\partial t} + \frac{\partial}{\partial \mathbf{r}}\left(\rho \mathbf{v} C - \left(D_t + D_b\right)\frac{\partial C}{\partial \mathbf{r}} \right) = S_C \qquad (11)$$

Here

r is the position vector in the domain (e.g. x and y in 2D Cartesian coordinates);

v is the velocity vector of the particulate cloud at position **r**;

D_t is the turbulent diffusion coefficient, zero in our case;

D_b is the Brownian motion diffusion coefficient, $K_B \delta_{ij} P_B$ in Equation 9;

S_C is the source term for aerosol supply, constant at the upstream boundary cells and zero for all other cells in the domain when t=0.

In the Eulerian approach, gas flow and particle motion are calculated simultaneously. A new particle cloud must be injected for each particle diameter of interest, and grid independence demonstrated. The Eulerian approach can be much slower than the Lagrangian approach. However, the problems with the Lagrangian approach discussed above, need to be resolved if the Lagrangian method is to be used reliably for all particle diameters.

GAS PROPERTIES

Gas Density, Viscosity and Mean Free Path

Simulations for filter media in the continuum regime with specified isothermal conditions can use constant values of thermophysical properties. Measured values for properties are preferable to values based on theoretical expressions. Dry and humid air properties are available from ASHRAE Handbook- Fundamentals (2009); NOAA/NASA (1976); and Jennings (1988). For other test gases, Yaws and Baker (2001) and the internet sites of industrial-gas suppliers are useful. Theoretical and empirical expressions and data for gas thermophysical properties, including extreme conditions, are given in Poling et al (2002), and Bird et al (2002). National laboratories in the U.K. and U.S. provide extensive equations and tables of gas properties. Values for gas properties of interest here obtained for several gases likely to require filtration are given in Part II of this paper.

Gas/Boundary TMAC Values

The TMAC at a given gas/solid boundary point is dependent on the gas involved, and its bulk temperature and pressure; the boundary material, and its temperature and surface roughness. TMAC calculation requires a relation between the terms of Equation 4 and the boundary geometry and experimental conditions. Measurements of TMACs have therefore been made using simple geometries with known analytical solutions to the governing equations for the flow regime present.

Values of TMAC have been obtained by measurements of flow through tubes; the sedimentation velocities of spheres; torque on rotating bodies; the decay rate of angular velocity for rotating bodies; force from impact of molecular beams; and physical adsorption. Agrawal and Prabhu (2008), Cao et al (2009), and Chew (2009) survey measurements of TMACs. Unfortunately, these experiments rarely provide TMACs for common filter media fiber and binder materials combined with gases usually filtered (e.g. ambient moist air). For the most part, they employ noble gases, low pressure, and materials like silicon. Table 2 lists values of σ_{tma} measured for various combinations of gas, solid surface, surface condition and Knudsen number range. In some cases, σ_{tma} has been calculated from the slip coefficient.

Particle Drag and Diffusion; Cunningham Correction

The aerodynamic drag and diffusion properties of both spherical and non-spherical particles have been widely studied. Brown (1993) discusses both, and Donley (1991) and Dahneke (1973) summarize studies of compact nonspherical particles. Cheng et al (1988) studied the drag of aggregate forms common in ambient air.

PARAMETER RANGES IN AIR FILTRATION

Media Fiber Diameter, Density and Fractional Volume

To calculate parameter ranges in the sections below, we have adopted a fiber diameter range of 10 - 100 μm. The actual size distribution of fibers in media being simulated must be measured, usually by analysis of scanning-electron-microscope (SEM) images. These typically resolve fiber diameters as low as 2 nm, and have sufficient depth-of-field that an image of an intact sheet of filter medium can represent the full depth of the medium. If the filter medium has intentionally graded fiber diameters or fractional solids, one must disassemble it to get a representative fiber sample. ASTM (2008b) describes this; Rivers and Murphy (2000) describe the simpler sheet-examination procedure and other media-characterization procedures.

Some fibrous media incorporate mixed fiber materials, and many include polymeric binders. Simulation of bonded media geometry requires values for the volumetric fraction of both components. Rivers and Murphy (2000) and ASTM (2008a) report values for these densities. Direct density measurement is preferable, because the exact polymer or glass type is rarely known.

Media Binder Content and Density

Polymeric binders may reach 20% of the solid volume of filter media. Polymers made from the same monomers, or copolymers, can have a range of densities. Media manufacturers are reluctant to reveal the specific materials used in their media, and measurement of the density of the actual binder may be necessary for accurate description of media geometry. Separation of polymeric binder from fiberglass is accomplished by enough heating to ignite the polymer, but not melt the glass (TAPPI 2010b). It may be possible to make fiber/binder separations with solvents which dissolve the binder and fiber selectively, or to pick them apart mechanically. The density of the separated solid material can then be determined using a pycnometer.

Fiber Reynolds and Knudsen Numbers

Media face velocities may range from about 0.015 m/s (for nuclear-grade ULPA filters) to about 4 m/s (for spun-fiber filters). Fiber diameters are much less for high-efficiency media than for low-efficiency media. The ranges of fiber *Re* and *Kn* to be expected for air from sea level and to 3000 m altitude, -40 °C to +70 °C are:

$$0.005 < \mathrm{Re} < 16 \quad \text{and} \quad 0.01 < Kn < 0.8$$

The high *Kn* values are in the transitional flow regime, so all filter operating conditions may not be reliably simulated using the Navier-Stokes equations, especially with media containing nanofibers. Reynolds numbers are all very low, indicative of laminar, “creeping” flow, even for the coarsest filter media operating at full duct velocity.

Media Thickness and Compression

Some air filter media, especially melt-blown fiberglass mats, are compressed significantly by airflow. The actual thickness of the filter medium with gas flowing through is needed to obtain the true fractional solid volume. Airflow compression can be simulated by loading a stiff metal plate covering a sheet of filter medium with successively increased mass. Several layers of media are often stacked to provide average values of thickness and compression. ISO (1995, 2005) and TAPPI (2010a) describe these methods.

Test Particle Diameter and Density

Particles used in tests for verifying CFD simulations need to have geometries as near as possible to those used in the simulations. Most simulations will be for spherical particles. The most reliable measurement of solid micro- and nano-sphere diameters is from electron microscope images. Aerosol differential mobility analyzers and aerodynamic particle size analyzers are somewhat less accurate. Laser scattering aerosol spectrometers are often used for speed and ease of operation, but are not able to measure diameters below about 90 nm, and are still less accurate than the other methods.

Verification for different particle densities as well as different diameters and media velocities lends credence to the CFD analysis. Table 3 lists densities for some laboratory-generated aerosols; all except sodium chloride, which is generally cubic, are essentially spheres.

Meaningful CFD verification requires error analysis, including the parameters media area, gas properties and flow rate, particle diameter, density, and upstream and downstream

particle counts. Sampling trains upstream and downstream of the filter medium must be identical to balance out the effect of particle losses in sampling probes and tubing.

Particle and Fiber Charges

Aerosol clouds used for laboratory efficiency measurements include some charged particles. These charges can be reduced by neutralizers, but not eliminated. A fully-neutralized cloud carries particle charges distributed according to the diameters of the particles, following the Boltzmann distribution, described in Hoppel and Frick (1990). Better realism in particle capture simulation should include charging of particles according to this distribution, and inclusion of an electrostatic image force in the Lagrangian simulation. This force is given in many sources, e.g. Brown (1993):

$$F_{ei} = \left(\frac{\varepsilon_f - 1}{\varepsilon_f + 1} \right) \frac{q^2}{4\pi\varepsilon_o \left(d_f - d_p \right)^2} \tag{12}$$

Here q is the particle charge in coulombs, ε_o the permittivity of free space, and ε_f the relative permittivity of the fiber. If electret-charged media are simulated, validation of simulations requires either neutralization of the electret medium or simulation of electrostatic forces.

SIMULATION OF FILTER MEDIA GEOMETRY IN FLOW DOMAINS

Simulations involve either 2D or 3D geometries representing a small part of a sheet of filter media. Simplification of actual media geometry is obviously necessary. Rief et al (2006) and Maze et al (2007), for example, created media descriptions in 3D with randomly oriented, randomly spaced circular cylinders with uniform diameters . Other 3D simulations have been for uniform fibers in regular arrays, which are far from reality. Lücke et al (1993), Bergman and Corey (1999), Tronville and Rivers (2008), and Zhou et al (2009) used 2D domains, sections cut through the simulated media. These 2D rectangular domains were populated with randomly located circles with random diameters having diameter distributions matching the distributions of the actual media fibers.

PUBLISHED SINGLE- FIBER AND POLYFIBER FLOW SIMULATIONS

CFD-based simulations of fibrous filter media pressure drop and particle capture have been performed at several levels of realism, beginning with single fibers, and progressing through regular, two-dimensional arrays of cylinders to randomly-located fibers with a distribution of fiber diameters. Three-dimensional models allow simulation of the random orientation of fibers, but the computational power needed for complete CFD modeling of actual fibrous media geometries appears thus far to be beyond the reach of air filter investigators. We feel that CFD modeling must at least incorporate the fiber diameter distribution present in the modeled media, and the presence of nearby fibers, both of which strongly influence the local motion of gas and particles. For these reasons, we include only multi-fiber simulations in Table 4. Many papers with numerical flow and particle-capture solutions offer validations based on

comparisons to earlier correlations based on “effective fiber diameters” derived from pressure drop measurements. The fit to these correlations may be impressive, but in the original referenced correlations errors of ±40% relative to measured values are not unusual. Other papers offer validation by comparison to other numerical solutions. Table 4 summarizes the conditions and results of some of the multi-fiber continuum flow simulations we have found in the literature. These include one, (Hosseini and Tafreshi 2010) which used the Navier-Stokes / finite volume combination with slip, but with $Kn \sim 0.66$ for all fibers. This is well beyond continuum flow, and would seem to require a different CFD approach.

IMPORTANT FACTORS NOT GENERALLY ADDRESSED IN SIMULATIONS

Particles which contact a filter fiber may bounce off the fiber. Particles which do adhere may come loose and re-enter the flowing gas. Their probability of detachment and recapture could be important. Dahneke (1995) analyzes these effects. Particles which do adhere to the fibers change the geometry of the computational domain. They also often become particle capture sites, forming fiber-like arrays called dendrites. This and other forms of media loading are beyond the scope of this paper. Some media compress significantly under operating pressure differences. These effects have been simulated, but much more study is needed to develop reliable simulations and to measure the needed media, fiber and particle parameters.

CONCLUSIONS

Performance of fibrous air filter media can be simulated using finite volume CFD and the Navier-Stokes equations, when Knudsen numbers based on fiber diameters are less than 0.01. Accommodation coefficients for filter fibers are almost impossible to predict; we suggest 0.93 as a starting value for CFD runs in the continuum regime, followed by a search for the value of accommodation coefficient which best predicts the measured pressure drops across the filter medium. For circular fibers, fiber boundary conditions must include terms related to boundary curvature. Particle capture calculations using Lagrangian techniques and incorporating Brownian motion are satisfactory for spherical particles, including nanoparticles. For nanoparticle capture, the equilibrium charge distribution and dielectrophoretic forces should be included. Discrepancies between simulated and measured results for filter media behavior can probably be improved if media binder and compression are simulated, and particle bounce and adhesion are modeled. 2D simulations use much less computation power and time than 3D simulations, hence are worth trying to study the present uncertainties in filtration and simulation theory. Simulation procedures must always be verified by comparison to experimental data on the media geometries and particle and gas properties simulated.

NOMENCLATURE

(Where no units are given, item is dimensionless)

t = time, s

k = Boltzmann const., 1.3806503 x 10^{-23} J/K

M = molecular weight, kg mol^{-1}

Kn = Knudsen number

r = radius, m

C_C = Cunningham correction (see Equation 8)

T = temperature, K

A = Avagodro const., 6.022142×10^{23} mol^{-1}

f = factor

u, **v** = vector velocities, m/s

S = Sutherland Constant, K

$\bullet$ = vector dot product operator

d = diameter, m

∇ = vector divergence operator

q = particle charge, coulombs

ε_o = permittivity of free space, farad/m

ε_f = relative fiber permittivity

g = acceleration of gravity, ms^{-2}

Greek Symbols

λ = molecular mean free path, m

ρ = density, kg/m^3

μ = absolute viscosity, Pa-s

Ω_λ = collision integral (Equation 12)

σ_{tma} = accommodation coefficient

θ = angle, radians

δ_{ij} = Kronecker's delta

α,β,γ = dimensionless constants (Equation 15)

Subscripts

p = particle

f = fiber

g = gas

in = incident

rf = reflected

REFERENCES

Agrawal, A. and S.V. Prabhu 2008. Survey of measurement of tangential momentum accommodation coefficients. J. Vac. Sci. & Tech A 26: 634-645.

Aliabadi, A.A., and S.N. Rogak. 2011. Letter to the Editor: Lagrangian Stochastic particle tracking. Aerosol Sci. & Tech. 45: 313-314.

Allen, M. D. and O. G. Raabe. 1985. Slip correction measurements of spherical solid aerosol particles in an improved Millikan apparatus. Aerosol Sci. and Tech. 4: 269-286.

Arkilic E.B., (1997) Measurement of the Mass Flow and Tangential Momentum Accommodation Coefficient in Silicon Micromachined Channels, Ph.D. thesis, Massachusetts Institute of Technology, Cambridge, MA USA.

ASHRAE, 2009. ASHRAE Handbook- Fundamentals. Atlanta USA: ASHRAE.

AIAA, 1998. Guide for the Verification and Validation of Computational Fluid Dynamics Simulations (AIAA G-077-1998e) www.aiaa.org

ASTM, 2008a. ASTM D629-08: Quantitative Analysis of Textiles. Philadelphia, USA : ASTM.

ASTM, 2008b. ASTM D2130-09 (2008) Standard Test Method for Diameter of Wool and Other Microfibers by

Projection. Philadelphia, USA: ASTM.

Barber, R.W., Y. Sun, X.J. Gu and D. Emerson. 2004. Isothermal slip flow over curved surfaces. Vacuum 76: 73-81.

Bergman, W. and I. Corey. 1997. Filtration theory using computer simulations. 24th DOE/NRC Nuclear Air Cleaning Conference Proceedings, 485-499.

Bird, G.A. 1994. Molecular Gasdynamics and Direct Simulation of Gas Flows. Oxford, UK : Oxford University Press

Bird, R. B., W. E. Stewart, and E.N. Lightfoot. 2002. Transport Phenomena, 2nd ed. Hoboken, NJ. USA, Wiley

Brown, R.C. 1993. Air Filtration: An Integrated Approach to the Theory and Application of Fibrous Filters. Oxford, UK: Pergamon Press.

Cai, J. 1992. Fibrous Filters With Non-Ideal Conditions. PhD Thesis, Kungliga Tekniska Högskolan, Stockholm.

Cao, B.Y., J. Sun, M. Chen, and Z.-Y. Guo. 2009. Molecular momentum transport at fluid-solid interfaces in MEMS/NEMS: A review. Int'l. J. Molecular Science: 4638-4706

Chapman, S., and T.G. Cowling. 1970. The Mathematical Theory of Non-Uniform Gases, 3rd Ed. London: Cambridge University Press.

Cheng, Y.S., M.D. Allen, D.P. Gallegos, H.C. Yeh, K. Peterson. 1988. Drag force and slip correction of aggregate aerosols. Aerosol Sci. & Tech. 8: 199-214.

Chew, A. D. 2009. Comment on "Survey on measurement of tangential momentum accommodation coefficient [J. Vac. Sci. Tech. A 26, 634 (2008)]." Journal of Vacuum Science & Technology A 27: 591-592.

Dahneke, B.E. 1973. Slip Correction Factors for nonspherical bodies – III. The Form of the General Law. J. Aerosol Science 4: 1973, 163-170.

Dahneke, B. E. 1995. Particle bounce or capture- search for an adequate theory: I. Conservation-of-energy model for a simple collision process. Aerosol Sci. & Tech. 23: 25-39

Donley, E. 1991. The drag force on a sphere. UMAP Journal 12: 47-80.

Ewart, T., P. Perrier, J. Graur, J. Meolans. Tangential momentum accommodation coefficients in microtubes. 2007. Microfluidics and Nanofluidics 3: 689-695.

Hoppel, W.A., and G.M. Frick. 1990. The nonequilibrium character of the aerosol charge distributions produced by neutralizers. Aerosol Sci. & Tech 12: 471-496.

Hosseini, S. A. and H. Vahedi Tafreshi. 2010. 3-D simulation of particle filtration in electrospun nanofibrous filters. Powder Technology 201: 153-160.

ISO. 1995. ISO 9073-2:1995. Textile Test Methods for Nonwovens - Part 2: Determination of Thickness. www.iso.org.

ISO. 2005. ISO 12625-3:2005. Tissue Paper and Tissue Products - Part 3: Determination of Thickness, Bulking Thickness and Bulk Density. www.iso.org.

Jang, J. and S.T. Wereley. 2006. Effective heights and tangential momentum accommodation coefficients of gaseous slip flows in deep reactive ion etching. J. Micromechanics and Microengineering 16: 493- 504.

Jennings, S.G. 1988. The mean free path in air. J. of Aerosol Sci. 19: 159-166.

Kirkpatrick, M.P., S.W. Armfield, and J.H. Kent. 2003. A representation of curved boundaries for the solution of the Navier-Stokes equations on a staggered three-dimensional cartesian grid. J.Comp. Phys. 184: 1-36.

Knefel, M. 2011. Structure and pressure drop of real and virtual metal wire meshes. Proc. Filtech 2011: vI-196-202.

Krivodonova, L. and M. Berger. High-order accurate implementaton of solid wall boundary conditions in curved geometries. J. Comp. Phys. 211: 492-512.

Lucas, K.,2007, *Molecular Models for Fluids*. Cambridge University Press, New York.

Lücke, T., C. Knösche, R. Adam, and R. Tittel, 1993. Calculation of fluid flow and particle trajectories in a system of randomly placed parallel cylinders – a new model for aerosol filtration. J. Aerosol Sci. 24: Supp.1 S555-S556.

Maze, B., H. Vahedi Tafreshi, Q. Wang, B. Pourdeyhimi. 2007. A simulation of unsteady-state filtration via nanofiber media at reduced operating pressures. J. Aerosol Sci. 38: 550-571.

Millikan, R.A., 1923. Coefficient of slip in gases and the law of reflection of molecules from the surfaces of solids and liquids. Phys. Rev. 21: 217-238.

NOAA/NASA, 1976. U.S. Standard Atmosphere U.S. Government Printing Office (downloadable from Wikipedia)

Poling, B.E., J.M. Prausnitz, J.P. O'Connell. 2002. The Properties of Gases & Liquids, 5th Ed. New York: McGraw-Hill.

Rao, N. and M. Faghri. 1988. Computer modeling of aerosol filtration in fibrous filters. Aerosol Sci. & Tech. 8: 133-

Rief, S., A. Latz, and A. Wiegmann. 2006. Research note: Computer simulations of air filtration including surface charges in 3-dimensional fibrous microstructures. Filtration 6: 169-172.

Rivers, R.D., and D.J. Murphy. 2000. Air filter performance under variable air volume conditions. ASHRAE Transactions 106 pt. 2: 31-144.

Seidl, M. and E. Steinheil. 1974. Measurement of momentum accommodation coefficients on surfaces characterized by auger spectroscopy, SIMS and LEED. Proc. 9th Int'l. Symp. Rarefied Gas Dynamics Porz-Wahn, Germany, DFVLR Press

TAPPI 2010a. TAPPI T-1006 sp-10 Testing of Fiber Glass Mats: Use of Modified TAPPI Procedures for Sampling and Lot Acceptance, Stiffness, Tear Resistance, Air Permeability and Thickness. www.tappi.org.

TAPPI 2010b. TAPPI T- 1013 om-06 Loss on Ignition of Fiber Glass Mats. www.tappi.org.

Tronville, P., R.D. Rivers, and B. Zhou. 2008. Particle capture by air filter media having truncated log-normal fiber diameter distributions and random spacing of fibers. Proc. 10th World Filtration Cong.: III: 132-136

Urquiza, J.M., A. Garon, and A. Fortin. 2008. Implementing slip boundary conditions on curved boundaries. Proc. 8th World Cong. on Computational Mechanics.

Wang, J., S.C. Kim, and D.Y.H. Pui. 2011. Carbon nanotube penetration through a screen filter: Numerical modeling and comparison with experiment. Aerosol Sci. & Tech 45: 443-452.

Wang, Q., B. Maze, H.Vahedi Tafreshi, and B. Pourdeyhimi. 2006. Nanoparticle filtration by virtual nonwoven media. Proc. Amer. Filtration and Separation Conf. 2006

Yaws, C.L. and W. Baker. 2001. Matheson Gas Data Book, 7th Ed. New York, McGraw-Hill.

Yun, K.Y., and R.K. Agarwal, 2002. Burnett simulations of flows in microgeometries. in Proc. 3rd Int'l. Fluid Mechanics Meeting, AIAA 2002-2870. www.aiaa.org

Zhao, B., C. Chen, and A.C.K. Lai. 2011. Letter to the Editor: Lagrangian stochastic particle tracking: Further discussion. Aerosol Sci. & Tech. 45: 901-902.

Zhou, B., V. Bertola, E. Cafaro, L. De Giorgi and P. Tronville. 2009. Effect of slip flow on the pressure drop in fibrous filters. Proc. Filtech 2009, www.filtech.de.

PART I TABLE 1:

Knudsen Number Range	*Flow Regime*	*Governing Equations and Computation Method*	Code
Kn approaches 0	Continuum Flow, no molecular diffusion (zero viscosity)	Euler Equations	A
$Kn < 0.001$	Continuum Flow, molecular diffusion (viscous gas)	Navier-Stokes Equations without slip	B
$0.001 < Kn < 0.01$	Continuum-Transition Flow	Navier-Stokes Equations with partial slip	C
$0.001 < Kn < 0.1$	Continuum-Transition Flow	Burnett Equations with partial slip	D
$0.1 < Kn < 1.0$	Transition Flow	Burnett Equations With partial slip	E
$0.1 < Kn < 1.0$	Transition Flow	Grad Moment Equations	F
$0.1 < Kn < 1.0$	Transition Flow	DSMC	G
$0.1 < Kn < 1.0$	Transition Flow	Lattice-Boltzmann	H
$Kn > 1.0$	Free-Molecular Flow	Collisionless Boltzmann	J
$Kn > 1.0$	Free-Molecular Flow	Molecular Dynamics	K

Code B is often referred to as the “no-slip” condition,

codes C through H as “partial-slip”, and codes J and K as “full-slip”.

PART I TABLE 2:

Ref.	*Gases*	*Surface*	*Surface Conditions*	*Rms Surface Roughness nm*	*Kn Range*	*Pressure Range kPa*	*Measured* σ_{tma}	*Method*
1	Ar	Silicon	etched, clean	~0.7	0.05 – 0.41	130-430	0.62 – 0.98	Channel
1	N_2,	Silicon	etched, clean	~0.7	0.05 – 0.35	132-430	0.83 – 0.95	Channel
1	CO_2	Silicon	etched,clean	~0.7	0.035 – 0.45	135-430	0.85 -1.26	Channel
2	Ar,He	silica tube	fused, clean	NG	0.003-0.3	NG	0.71 – 0.91	Tube
2	N_2	silica tube	fused,clean	NG	0.003-0.3	NG	0.77 – 0.91	Tube
3	Air	glass, silicon	fused, etched, clean	2 – 30	0.002–0.1	98.5	~0.85	Channel
4	He	copper	Some as received, some polished	2500	0.08-314	NA	0.67-1.08, 70º-10º Incident.angle	Molec-ular. Beam
5	Air	PVC, PVT	surfactant-free	~5	0 – 0.2	57-102	0.934	Sphere fall
5	Air	PVC, PVT	surfactant-free	~5	1.0	~13	0.857	“
5	Air	PVC, PVT	surfactant-free	~5	10	~2	0.756	“
6	Air	Oil	Liquid	0.1?	0 – 0.2	50-100	0.928	“
6	Air	Oil	Liquid	0.1?	1.0	~10	0.828	“
6	Air	Oil	Liquid	0.1?	10	~2	0.770	“

PVC = Polyvinyl chloride spheres; PVT = Polyvinyl toluene spheres; NG=not given; NA=not applicable

References: [1] Arkilic 1997; [2] Ewart, Perrier, Graur and Méolans 2007; [3] Jang and Wereley 2006; [4] Seidl and Steinheil 1974; [5] Allen and Raabe 1985; [6] Millikan 1923 (as recalculated by [5])

PART I TABLE 3:

Particle Material	Density, kg/m^3
Polystyrene Latex	1050
DEHS(†)	900-920
Oleic Acid	894
Stearic Acid	941
Sodium Chloride	1860-2180
Potassium Iodide	3120
Methylene Blue	1340-1370
Polyvinyl Toluene	1040
Iron Oxide	2550
Sintered Fly Ash	3830

Silver	10500

(†) DEHS= di-ethylhexl sebacate

= bis(2-ethylhexyl decanedioate)

PART I TABLE 4:

Ref.	Media Form	Gas, Pressure	CFD Method	Validation Method	Particle	Particle Tracking	Results Given
1	2D RanF/RanL, 3D UFD, Reg	Air, Norm	NS	NG	UPD	Lagrangian + Brownian	Eff, PD
2	2D/SF 3D/SF	Air, Norm	KuwaC	NG	2D/Rngpd 3D/UPD	Lagrangian + Brownian	Eff
3	2D/Reg/Elect Rectangular	Air, Norm	NS	Cregr	Rngpd, Charged, Neutralized	Lagrangian + Brownian	Eff
4	3D/UFD/RanL	Air, Norm	NS, slip	Cregr	Rngpd	Lagrangian, Euler	Eff, PD
5	3D/UFD/woven	Air, Norm	NS, no-slip	Cdata	Rngpd	Lagrangian	
6	2D/RanF/RanL	Air? Norm?	NS, slip	Cregr	UPD	Lagrangian + Brownian	Eff, PD
7	2D/UFD/Reg	Dimless	NS no-slip	Cregr	Dimless	Lagrangian + Brownian	Eff, PD
8	2D/RanF/RanL	Air, Norm	NS	Cdata	NG	NG	PD
9	3D/UFD/RanL	Air, Norm	NS, no-slip	Cregr	Rngpd	Lagrangian	Eff, PD
10	3D/UFD	Air?	NS, no	Cdata	Nanotubes,	Lagrangian	Eff,

		Norm?	fiber slip		PSL - UPD		PD

UFD: uniform fiber diameter NG: not given 2D: 2 Dimensional

UPD: uniform particle diameter NS: Navier-Stokes 3D: 3 Dimensional

RanL: fibers located randomly Elect: electret (charged) fibers FDrag: Fiber drag

RanF: random fiber diameters KuwaC: Kuwabara cell PD: pressure drop

Reg: fibers in a regular array Rngpd: Particle diameter range Eff: Efficiency

Norm: normal pressures, ~ 1 bar Dless: Results are for dimensionless ratios, e.g. as *f* (Pe, Stk).

Cdata: Compared to own test data Cregr: Compared to earlier data-fitted regression equations

References: 1: Bergman (1997); 2: Cai(1992); 3:Cao et al (2004); 4: Hosseini and Tafreshi (2010);

5: Knefel (2011); 6: Lücke et al (1993); 7:Rao & Faghri (1988); 8: Tronville et al (2008);

9: Wang et al (2006); 10: Wang et al (2011)

PART I FIGURE CAPTIONS:

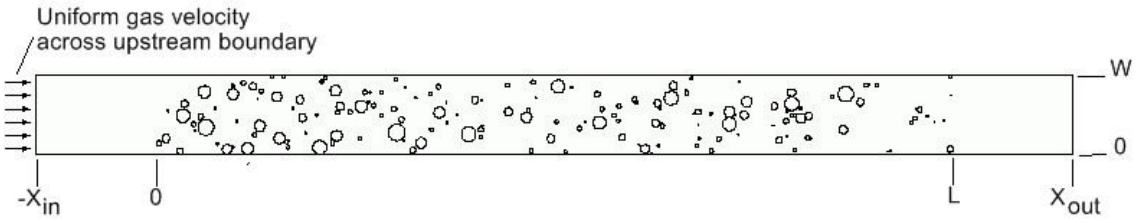

Figure 1. Typical 2-Dimensional Flow Domain for CFD Simulation of Fibrous Filter Media

PART I TABLE CAPTIONS:

Table 1. Flow Regimes, Knudsen Number Bounds, and Computational Methods

Table 2. Some Measured Tangential Momentum Accommodation Coefficients (TMAC)

Table 3. Reported Densities of Spherical and Nearly Spherical Test Aerosols

Table 4. Some Navier-Stokes Based Simulations of Multi-Fiber Air Filter Media

